FILTERING SURFACE WAVES

Choon Byong Park, Richard D. Miller, and Julian Ivanov
Kansas Geological Survey, Lawrence, Kansas

Summary

As surface waves become more commonly utilized in near-surface seismic investigations, the necessity of filtering them in the level of different modes often arises. This is because the surface wave application is usually based on the analysis of the fundamental mode only, whereas the surface waves as experienced during field surveys often are mutimodal in nature with higher modes dominating at high frequencies. This domination inevitably limits the analyzable bandwidth of the fundamental mode at the corresponding frequency band. In addition, the phase velocity range of higher modes often overlaps with that of the fundamental mode, making the conventional pie-slice f-k filtering ineffective for the purpose of filtering higher modes only. Two approaches are introduced. One implements in the frequency-wave number (f-k) space by redefining the rejection zone as narrow and curved (bow-slice) instead of the familiar pie-shaped zone. The other accomplishes the necessary filtering by utilizing the frequency-variant linear move out (FV-LMO) correction made from the dispersion information of the higher mode previously analyzed. These two approaches can also be useful during reflection processing.

Introduction

Seismic surface waves (Rayleigh or Love waves) are dispersive when the velocity of the propagating medium changes with depth. This is seen most clearly during the near-surface seismic surveys investigating shallow earth materials whose seismic velocity changes very rapidly with depth. Naturally enough, this dispersive nature of surface waves is often utilized to infer the seismic velocity (S-wave velocity, Vs) structure of the near-surface materials. For example, the multichannel analysis of surface waves (MASW) method (Park et al., 1999; Xia et al., 1999; Miller et al., 1999) aims at this by analyzing seismic data acquired from the mutichannel recording method. MASW usually uses the fundamental mode of surface waves as the primary signal whose dispersion curve is obtained first and then passed into the inversion process to calculate the most probable Vs profile. To generate a Vs profile of a wide depth range, it is essential to prepare a broadband dispersion curve. From the general perspective of inversion theory, the high frequency (e.g., > 20 Hz) portion of the dispersion curve takes on a greater importance because it directly influences the resolution of the shallow Vs's that in turn influence the resolution at a deeper level. However, strong higher modes of surface waves often dominate at this range of frequency and make the extraction of the fundamental-mode curve difficult or impossible (Park et al., 2000). The velocity filter (or pie-slice f-k filter) (Sheriff and Geldart, 1982) could be used to alleviate the domination before the dispersion curve analysis. However, this becomes necessary only when the phase velocity range of the higher modes is so different from that of the fundamental mode that the zones of rejection and passing are clearly separated in the frequency-wave number (f-k) space. Higher modes observed during normal MASW surveys indicate that they quite often overlap the fundamental mode in the phase velocity range (Figure 1).

Surface wave filtering is often applied during reflection processing also because the strong surface waves would dominate over the weak reflection signals and mask them. When the velocity of the body wave is significantly different from that of the surface wave, as is the case with most P-wave reflection data, then the conventional pie-slice (f-k) filter would be quite effective. However, when the body-wave velocity becomes comparable to that of the surface waves, as is the case with the S-wave

reflection surveys, the pie-slice processing may filter out not only the surface (Love) waves but also the flank side of the reflection hyperbola at far-offset traces.

The necessity of filtering surface waves in a more delicate manner than conventionally practiced calls for refinement of existing schemes or development of new schemes. In this paper, the conventional pie-slice f-k scheme is refined in such a way that the rejecting zone in f-k space is no longer a pie shape, but a narrow curved shape (a bow) that follows a trajectory in the f-k space. The trajectory is defined from the dispersion information of the rejecting event that is obtained through a normal dispersion analysis in the MASW method. New approaches are also introduced that utilize the frequency variant linear move out (FV-LMO) correction by Park et al. (1998a).

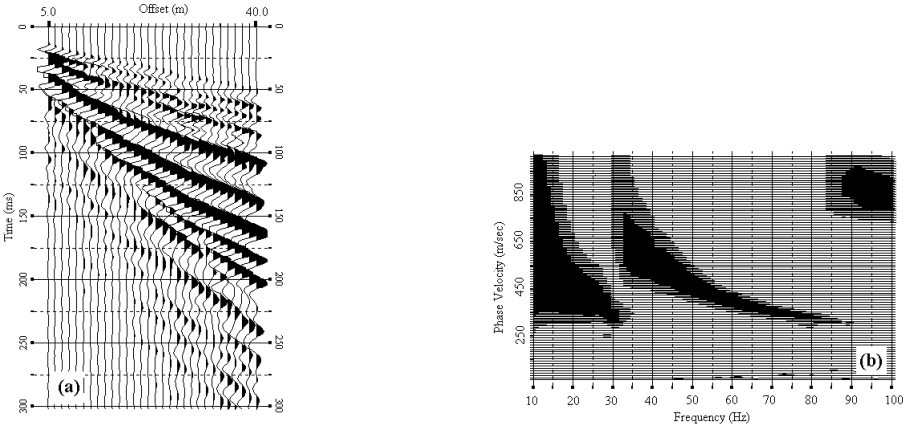

Figure 1. (a) A multichannel seismic record (shot gather) collected at a desert site near Yuma, Arizona, using a weight-drop source and 10-Hz geophones, and (b) dispersion curve image constructed from this shot gather by using a method by Park et al. (1998b).

Overview of Candidate Methods

The key point of surface-wave filtering under discussion is the capability to separate surface waves of different modes from each other as well as from body-wave events. Considering the linear surface waves on a mutichannel record, the linear move out (LMO) approach by the slant-stack (τ-p) method (Treitel et al., 1982) appears tempting. This would be an excellent choice to filter out surface waves against body waves of much higher velocities or to filter out the higher modes occurring in different velocity range than that of the fundamental mode. However, it cannot handle overlapping velocity ranges between different modes of surface waves or between surface- and body-wave events. In addition, it is not an operation perfectly reversible, sometimes requiring application of other optimization operations such as a rho filter (Claerbout, 1985). The limitation of this method in handling overlapping velocity ranges does not exist with its modification (the ω-p method) by McMechan and Yedlin (1981). Although not investigated in this study, this is another approach we will test in the future. However, the issue of imperfect reversal still remains, and this may cause a slight distortion of phase in the filtered data. During early MASW development, Park et al. (1998b) developed a f-C_f method that transforms total seismic wavefields of original field data directly into the frequency (f)-phase velocity (C_f) domain so that multimodal dispersion curves are imaged by loci of energy accumulation. This method, however, is also not perfectly reversible. Refinement of this method to make it reversible is currently under investigation. The only perfectly reversible operation commonly used in seismic processing is the

Fourier transformation. In addition, the issue of the overlapping velocity ranges between different seismic events can be solved when a double (2-D) Fourier transformation is applied into the time-space (t-x) axes. However, the way the conventional pie-slice method of f-k filtering defines the rejection zone must be refined, as we explain in the following section. Other approaches newly introduced are based on the notion that the phase shift of surface waves caused by dispersion can be removed by applying the same amount of shift with the opposite sign when the phase velocity information is available.

Bow-Slice *F-K* Filter

In conventional pie-slice f-k filtering, the rejection (filtering) zone is defined in frequency-wave number (f-k) space by two fanning linear slopes (thus called pie) of S_{max} and S_{min} determined from the two limiting velocities of C_{min} and C_{max}, respectively, as follows (and indicated by the solid line in Figure 4):

$$S_{\max} = \left.\frac{dk_x}{d\omega}\right|_{\max} = \frac{1}{C_{\min}}, \text{ and } S_{\min} = \left.\frac{dk_x}{d\omega}\right|_{\min} = \frac{1}{C_{\max}}. \quad (1)$$

On the other side, in bow-slice filtering the filtering zone is defined as a thin and curved zone whose locus, $\{\omega; k_x\}$, meets the following criterion (indicated by the dotted line in Figure 4):

$$\frac{\omega}{k_x} = C_\omega, \quad (2)$$

where C_ω is the phase velocity at frequency ω of the event to be filtered. C_ω may be the phase velocity of the first higher (C_ω^1) or the fundamental (C_ω^0) mode. This locus is usually not a straight line because of the dependency of the phase velocity (C) on the frequency (ω). It is assumed that C_ω is already known, as determined from a dispersion analysis. The actual shape of the bow slicing needs to be a certain band (with smooth tapering applied along the boundary) instead of a true line to avoid the Gibb's phenomenon. Width of the band is usually set being proportional to phase velocity.

Two dispersion curves (Figure 2) are used to model the surface-wave shot gathers in Figure 3. Both curves show the phase velocities mostly overlapping in the range of 200-650 m/sec. In fact, these curves are the ones obtained from analysis of the field data shown in Figure 1a by using the filtering schemes introduced in this paper. Modeled shot gathers in Figures 3a and 3b contain the fundamental mode only and both modes, respectively, of the dispersion curves shown in Figure 2. No body waves are included. In the multimodal case of Figure 3b, the higher mode was assigned an overall energy approximately twice that of the fundamental mode. Dispersion curve images corresponding to each shot gather obtained by using the method by Park et al. (1998b) are shown in Figures 3c and 3d. The multimodal image (Figure 3d) indicates that the strong higher mode energy completely dominates the fundamental mode at frequencies higher than about 30 Hz and therefore extraction of the corresponding part for the fundamental curve (dotted line) is almost impossible. The conventional pie slicing f-k method would inevitably filter out both modes because of the overlapping velocity range (Figures 5a and 5c). In the f-k spectrum (Figure 4) the fundamental mode is not visible at frequencies higher than about 30 Hz due to the dominance by the higher mode. When the rejection zone in the f-k spectrum is redefined as a narrow bow-shaped zone, only the energy from the higher mode is filtered out with that from the fundamental mode remaining almost intact (Figures 5b and 5d). Small amounts of artifacts are noticeable at high (> 80 Hz) frequencies in Figure 5d due to an incomplete rejection during the bow

slicing. An example with field data is shown in Figure 6. A 30-trace shot gather collected at a desert site near Yuma, Arizona, shows dominance of the higher mode at the high (> 30 Hz) frequencies (Figure 1). As shown in Figure 1b, the fundamental and higher modes have an overlapping range (approximately 200-650 m/sec) of phase velocity. When a pie slice is applied to this velocity range, the filtered output (Figure 6a) shows only body-wave events of higher velocities, completely missing both modes of surface waves (Figure 6c). The output from the bow slicing (Figure 6b), however, shows the fundamental mode being extended to as high as 80 Hz due to the selective filtering of the higher mode only (Figure 6d).

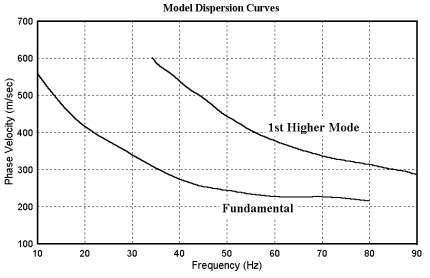

Figure 2. Dispersion curves of fundamental and the first higher modes that are used for modeling purposes.

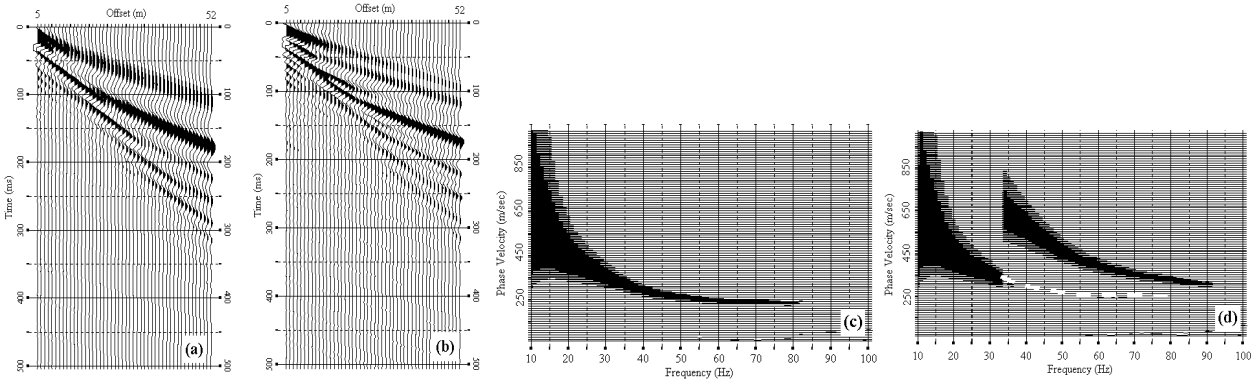

Figure 3. Synthetic shot gathers of (a) fundamental-mode only and (b) both modes of surface waves shown in Figure 2. Corresponding dispersion curve images are shown in (c) and (d), respectively.

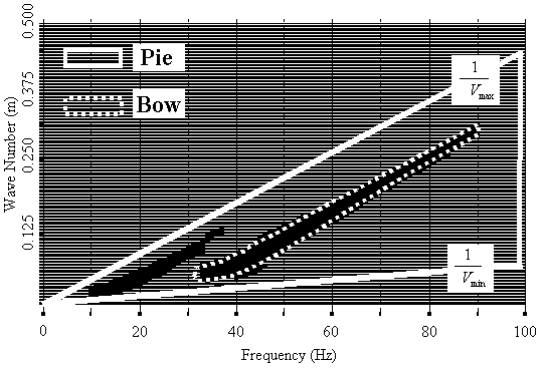

Figure 4. Frequency-wave number (f-k) amplitude spectrum of the shot gather in Figure 3b. Energy of the fundamental mode is not noticeable at high (> 30 Hz) frequencies due to the domination by the higher mode (dotted line).

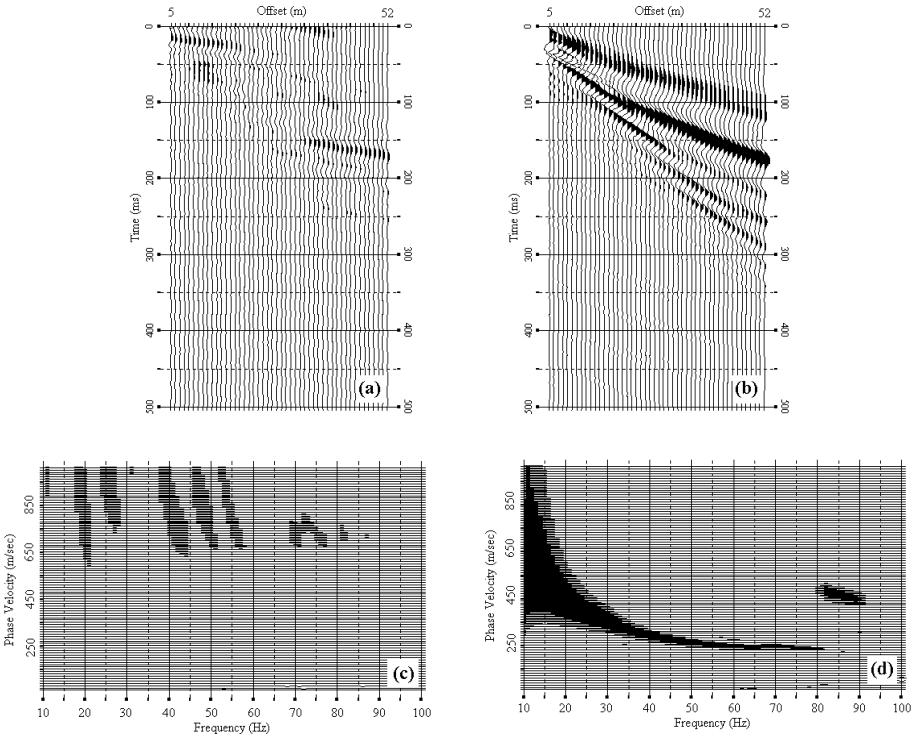

Figure 5. (a) Conventional pie-slice, and (b) bow-slice f-k filtering of the shot gather in Figure 3b. Corresponding dispersion curve images are shown in (c) and (d), respectively.

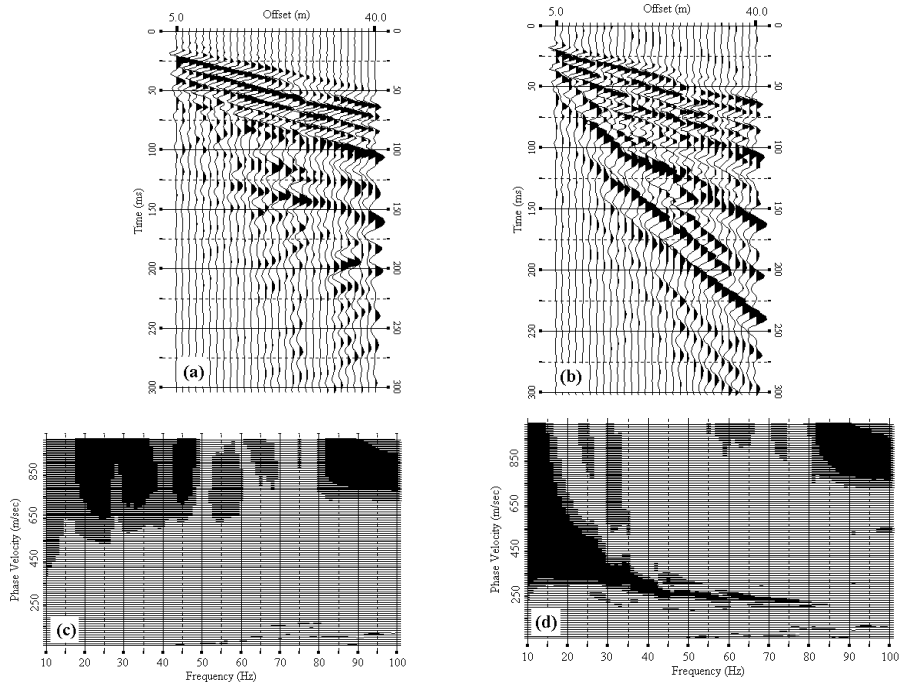

Figure 6. (a) Conventional pie-slice, and (b) bow-slice f-k filtering of the field shot gather in Figure 1a. Corresponding dispersion curve images are shown in (c) and (d), respectively.

Frequency Variant Linear Move Out (FV-LMO)

When the phase velocity information is available for a dispersive event, the dispersed waveform can be collapsed into an impulsive form through a frequency variant linear move out (FV-LMO) correction by Park et al. (1998a). The FV-LMO is a perfectly reversible operation as it takes place with the 1-D Fourier transformed data, $P(\omega,x)$, of a time-offset data, $p(t,x)$. It compensates for the phase shift, $\phi_+(\omega,x)$, caused by the dispersion property by applying an opposite amount (i.e., of the opposite sign) of phase shift, $\phi_-(\omega,x)$, to each frequency component (ω) of the trace at offset x:

$$P_{FV-LMO}(\omega,x) = \phi_-(\omega,x)P(\omega,x), \tag{3}$$

where $P_{FV-LMO}(\omega,x)$ is FV-LMO corrected $P(\omega,x)$, and $\phi_-(\omega,x)$ is defined as follows (Park et al., 1998a):

$$\phi_-(\omega,x) = e^{-jx\omega/C_\omega}. \tag{4}$$

This operation will also compensate for the offset effect, aligning all the collapsed waveforms at zero time. Then, rejection of the event to be filtered is accomplished by removing this collapsed event. Two

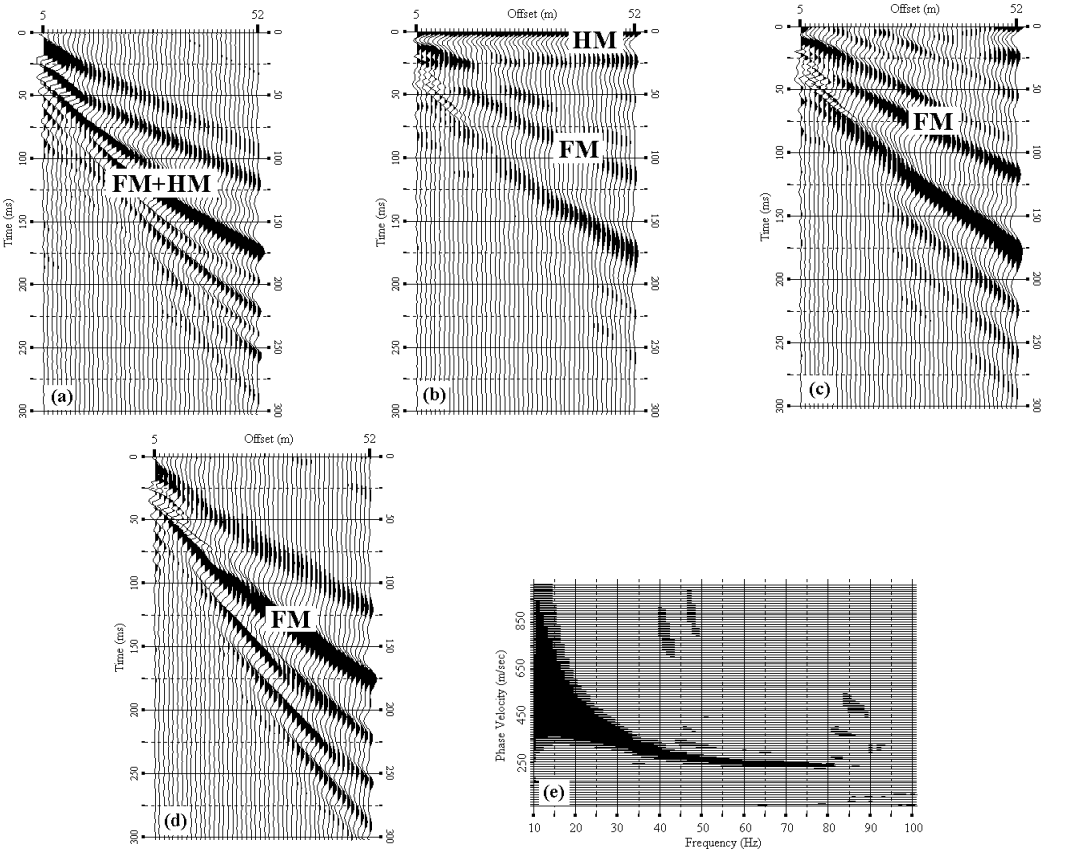

Figure 7. (a) Synthetic shot gather of both fundamental (FM) and higher (HM) modes, (b) frequency variant linear move out (FV-LMO) corrected (ϕ_-) using the phase velocity information (C_ω^1) of the HM, (c) zero-dip f-k filtering, (d) another FV-LMO correction (ϕ_+), and (e) the dispersion curve image for (d).

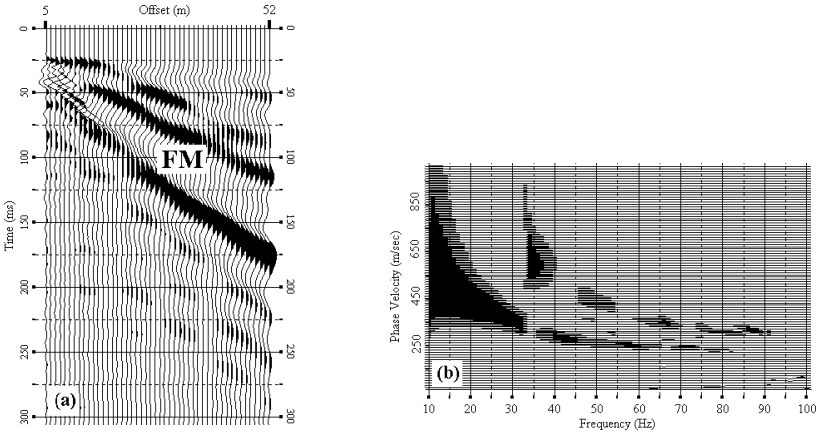

Figure 8. (a) Muting applied to reject the higher mode energy (HM) in Figure 7b, and (b) the dispersion curve image for (a) after another FV-LMO correction (ϕ_+) has been made. Compare Figure 8b with Figure 7e.

approaches are available to perform this rejection: zero-dip f-k filtering or time-domain muting. The former is preferable because the latter would inevitably cut out some of the signal energy.

The filtering scheme outlined above is illustrated by using synthetic data (Figure 7). The multi-modal shot gather in Figure 7a contains both fundamental (FM) and higher (HM) modes of surface waves from the dispersion curves displayed in Figure 2. When the FV-LMO is applied by using the first higher-mode phase velocity (C_ω^1) to define $\phi_-(\omega,x)$ in equation (4), the higher mode is collapsed and aligned along the zero-time line, whereas the fundamental mode is still dispersive (Figure 7b). The negative-time portion of this collapsed event would have appeared at the bottom (1000 ms) of the section. After the higher mode is rejected by using the zero-dip f-k filter, only the fundamental mode remains (Figure 7c). Then, another FV-LMO using $\phi_+(\omega,x)$ completes the entire procedure (Figure 7d). An image of the dispersion curve now confirms the successful rejection of the higher mode (Figure 7e). Muting (instead of zero-dip f-k filtering) shows a less complete performance due to the loss of information caused by the mute (Figure 8). The field data earlier used to illustrate bow slicing now has been filtered by this method and displayed in Figure 9. Results obtained by using both the zero-dip f-k filter (Figure 9a) and the time-domain mute (Figure 9b) are presented for comparison.

Possible Application to Reflection Processing

When a reflection event has a normal move out velocity comparable to the linear velocity of a surface wave event, the filtering methods explained in the previous two sections are applicable. This will be the case with S-wave reflection processing when the flank side at far-offset traces of the reflection hyperbola slopes almost identically to that of the surface wave event. This can also be the case with a P-wave reflection that originates from the top of a very shallow bedrock above which the overburden exists with a P-velocity comparable to the surface wave velocity of the bedrock. The reflection (marked as R) in Figure 10a shows its flank side that has a slope comparable to that of the surface wave event (marked as S) modeled by using the fundamental mode in Figure 2. The pie-slice f-k filter to reject the latter event would leave only the near-offset portion of the hyperbola (Figure10c), whereas the bow-slice f-k filter would leave most of it intact (Figure 10d). In both cases, some computational artifacts (A) are noticeable.

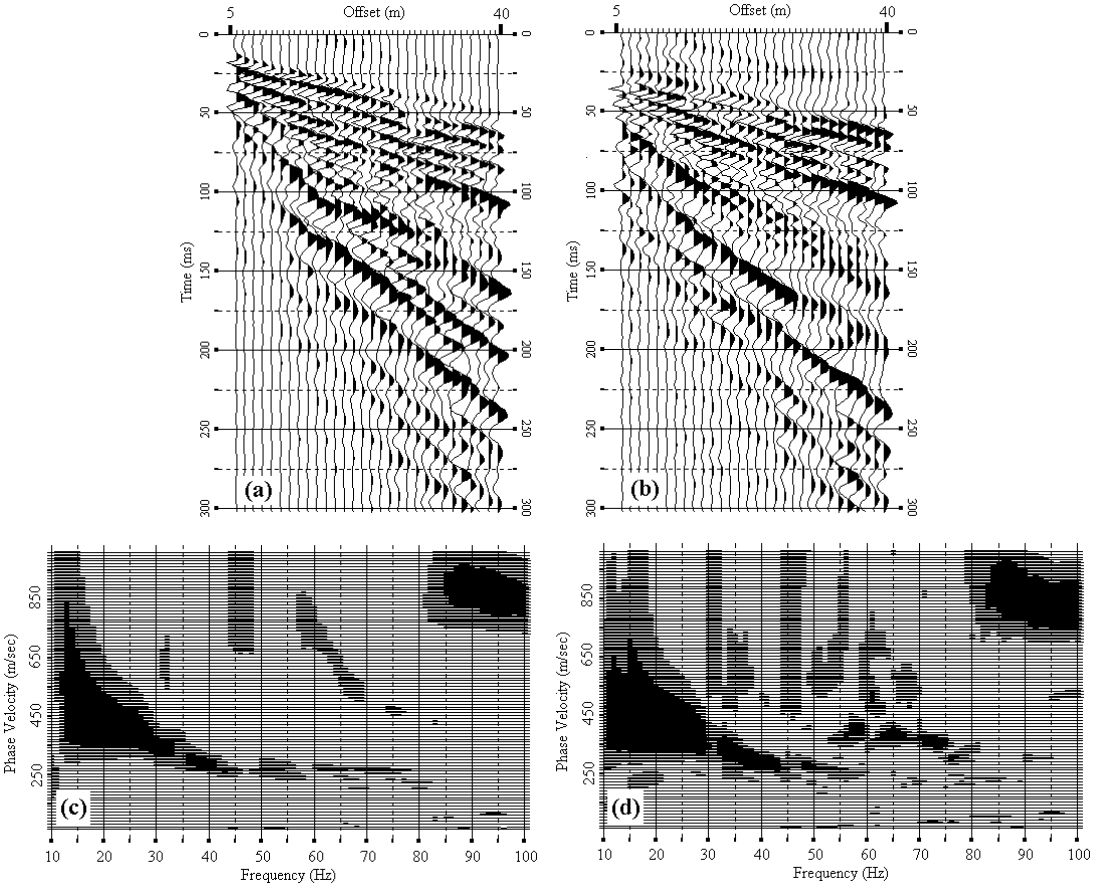

Figure 9. Results from the FV-LMO method using (a) the zero-dip f-k filter and (b) the time-domain mute to reject the collapsed energy of the higher mode. Corresponding dispersion curve images are shown in (c) and (d), respectively.

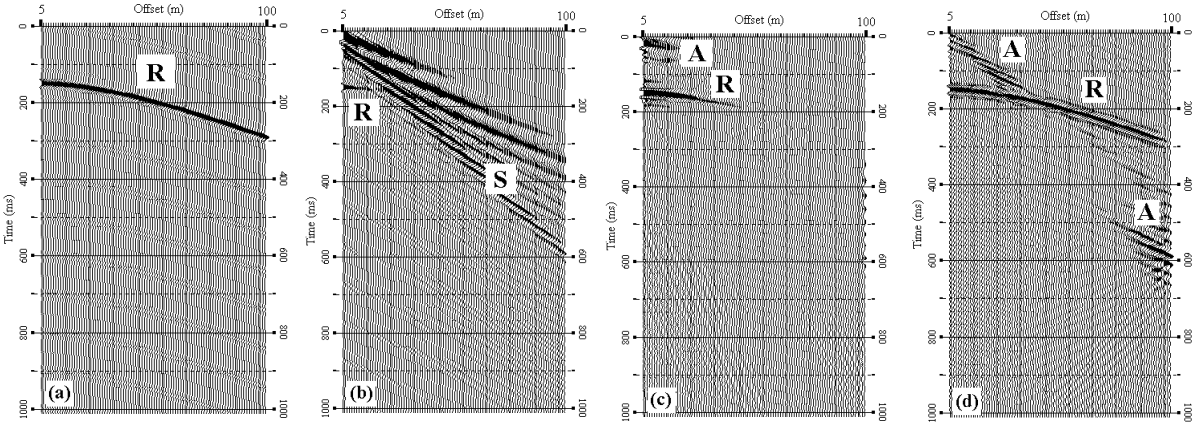

Figure 10. Synthetic shot gathers containing (a) a reflection hyperbola and (b) both reflection and a surface-wave event. Outputs by using (c) pie-slice and (d) bow-slice f-k filtering of (b).

An example of using the FV-LMO correction is shown in Figure 11. When the correction is applied using $\phi_{-}(\omega,x)$, the dispersive surface waves are collapsed into an impulsive (non-dispersive) event aligned along the zero-time line, whereas the originally impulsive reflection event has become dispersive (Figure 11a). Once this aligned event is rejected by using the zero-dip f-k filter, the dispersive reflection is visible with some artifacts (A) from the filtering (Figure 11b). The reflection hyperbola is recovered after the opposite FV-LMO correction of $\phi_{+}(\omega,x)$ is applied (Figure 11c). When the time-domain mute is applied instead of the zero-dip f-k filter (Figure 11d), the result is less complete because some of the reflection information has been rejected by the mute (Figure 11e).

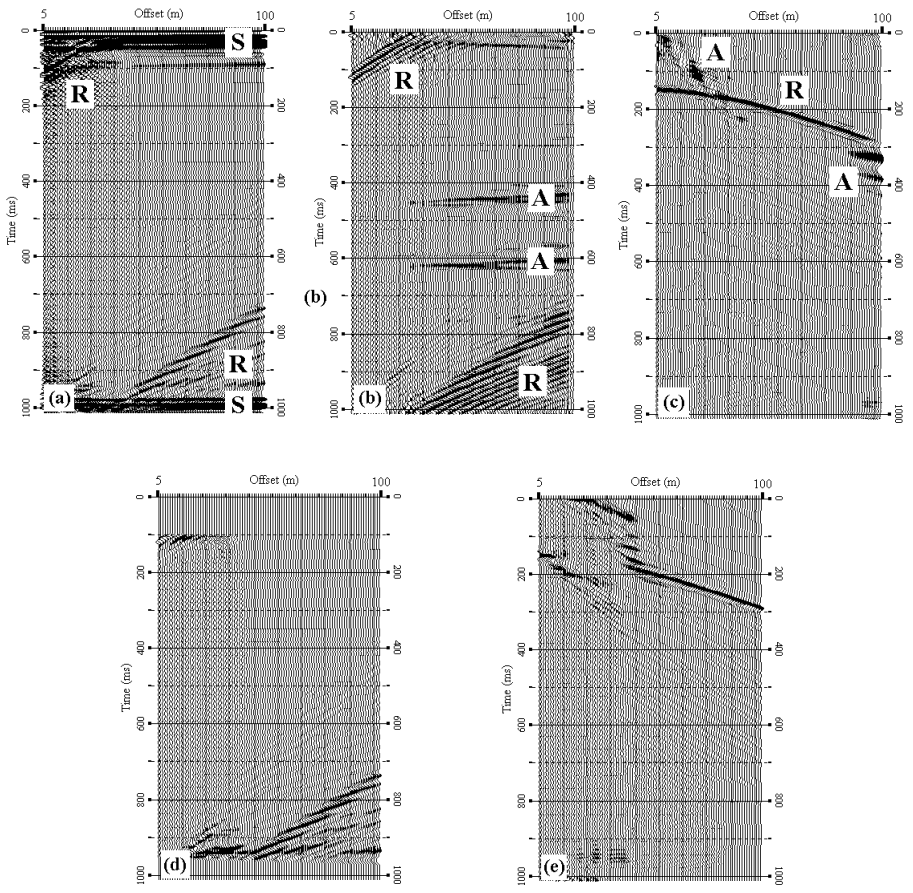

Figure 11. Shot gather shown in Figure 10b after (a) FV-LMO correction (ϕ_{-}), then (b) zero-dip f-k filtering, and then (c) another FV-LMO correction (ϕ_{+}) has been applied. The case of muting (instead of zero-dip f-k filtering) is shown in (d) and its result with the FV-LMO correction (ϕ_{+}) is shown in (e).

Discussion and Conclusions

Although description of the two different methods, bow slicing in the f-k space and the FV-LMO correction, are relatively straightforward, the width of the rejection zone and the tapering around it may significantly affect the overall performance of filtering. In the bow-slice method we mentioned that the width of the f-k space may be set to be proportional to the phase velocity. However, it may need to change with frequency, depending on the closeness of the rejected energy to the nearby signal energy

that will be preserved. Application of these two methods to reflection processing with a field data set was not attempted in this paper and will be presented in a future publication. Considering nowadays the growing importance of S-wave reflection surveys in near-surface seismic investigations, testing these methods using real field data is imperative.

The following conclusions are made:

1. As far as the phase velocity information can be extracted for the dispersive seismic event that is to be filtered out, the conventional pie-slice f-k filtering is not recommended because of excessive filtering that would often reject portions of the seismic data signal. Instead, a more delicate method like the bow-slice f-k filtering or a method utilizing the frequency variant linear move out (FV-LMO) correction would be more effective because of the elaborate definition of the rejection zone in either f-k or f-x domain.
2. Further improvement in the filtering performance may be expected when the rejected zone in the bow-slice method is re-filled by the information interpolated from the intact ambient (either 1-D or 2-D) data. This seems possible because the rejection is applied only to a small portion of the entire set of data.

Acknowledgments

We thank Mary Brohammer for her assistance in preparation of this manuscript.

References

1. Claerbout, J.F., 1985, Fundamentals of geophysical data processing: Blackwell Scientific Publications, California, 274 pp.
2. McMechan, G.A., and Yedlin, M.J., 1981, Analysis of dispersive waves by wave field transformation: Geophysics, 46, 869-874.
3. Miller, R.D., Xia, J., Park, C.B., and Ivanov, J., 1999, "Multichannel analysis of surface waves to map bedrock," The Leading Edge, 18(12), 1392-1396.
4. Park, C.B., Miller, R.D., and Xia, J., 1999, Multichannel analysis of surface waves (MASW): Geophysics, 64, 800-808.
5. Park, C.B., Miller, R.D., and Xia, J., 1998a, Ground roll as a tool to image near-surface anomaly: Technical Program with biographies, SEG, 68th Annual Meeting, New Orleans, Louisiana, 874-877.
6. Park, C.B., Miller, R.D., and Xia, J., 1998b, Imaging dispersion curves of surface waves on multichannel record: Technical Program with biographies, SEG, 68th Annual Meeting, New Orleans, Louisiana, 1377-1380.
7. Park, C.B., R.D. Miller, and J. Xia, 2000, Detection of higher mode surface waves over unconsolidated sediments by the MASW method: Proceedings of the Symposium on the Application of Geophysics to Engineering and Environmental Problems (SAGEEP 2000), Arlington, Va., February 20-24, p. 1-9.
8. Sheriff, R.E., and Geldart, L.P., 1982, Exploration seismology, volume 1: Cambridge University Press, 253 pp.
9. Treitel, S., Gutowski, P.R., and Wagner, D.E., 1982, Plane-wave decomposition of seismograms: Geophysics, 47, 1375-1401.
10. Xia, J., Miller, R.D., and Park, C.B., 1999, Estimation of near-surface velocity by inversion of Rayleigh wave, Geophysics, 64, 691-700.